STRESS ANALYSIS OF THICK PRESSURE VESSEL COMPOSED OF INCOMPRESSIBLE HYPERELASTIC MATERIALS

Yavar Anani[1] and Gholamhosein Rahimi[2]

[1,2]Mechanical Engineering Department, TarbiatModares University, Tehran, Iran,
Corresponding Author

ABSTRACT

In this paper, exact closed form solutions have been derived for stresses and the stretches in thick spherical shells made of hyperelastic material subjected to internal and external pressures. Stresses and displacements have been obtained for axisymmetric radial deformation for a spherical shell. Hyperelastic behavior is modeled by using Neo-hookean strain energy function. Material constant of strain energy function calculated from experimental data by least square method. As a result, distributions of extension ratio and stress components through the shell thickness have been presented. Sensitivity of stress components and displacement field to applied pressure and to outer to inner radius ratio of vessel has been investigated. Furthermore, the effects of structure parameters have been discussed in detail for different examples. Results demonstrate value of outer to inner radius ratio is a useful parameter from a design point of view which can be tailored to specific applications to control the stress.

KEYWORDS

Thick-walled spherical shells, hyperelastic material, finite deformation, Radial expansion/contraction

1. INTRODUCTION

The principal problem in the elasticity theory is to find the relation between the stress and the strain in a body under certain external forces. In small deformation, linear elasticity and Hooke's law is applied to find stress-strain relation. Under large deformation, materials show nonlinear elastic behavior which can be characterized by hyperelasticity. Rubber and rubber-like materials are assumed incompressible hyperelastic materials. Because of specific application characteristics and economic advantages of rubber and rubber-like materials, the corresponding structures, such as tubes, rings, shells, spheres and pads, composed of these materials, are widely used in petrochemical, aerospace, biomedical and many other fields of human life. Simple constitutive relations for studying their mechanical behavior include the neo-Hookean and the Mooney–Rivlin. Modeling the mechanical behavior of rubber-like materials within the framework of nonlinear elasticity theory has been the subject of intense investigations, which could be found in the review articles contributed by Beatty[1], Horgan and Polignone[2], Attard[3] and the monograph contributed by Fu and Ogden[4]. In recent years several researches were done on constitutive modeling of rubber like materials such as work ofDarijani, Carroll, Drozdov and Steinmann [5-8].The main concern of this paper is thick spherical shell made of rubber like materials, therefore studies and investigations on different axisymmetric shells are carefully reviewed and their key notes are mentioned here. Shells are common structural elements in many engineering applications, including pressure vessels, sub-marine hulls, ship hulls, wings and fuselages of airplanes, missiles, automobile tires, pipes, exteriors of rockets, concrete roofs,

DOI : 10.14810/ijmech.2015.4303

chimneys, cooling towers, liquid storage tanks, and many other structures. They are also found in nature in the form of eggs, leaves, inner ear, bladder, blood vessels, skulls, and geological formations [9]. Explicit solutions for radial deformations of a cylinder composed of a homogeneous Mooney–Rivlin material was given by Rivlin [10], who also investigated the eversion of a cylindrical tube. Inflation and bifurcation of thick-walled compressible elastic spherical shells was studied by Haughton[11]. In another study, Abeyaratne and Horgan investigated, in some detail, the deformation of pressurized thick-walled spherical shells composed of compressible harmonic elastic material. They presumed that the spherical shape was maintained sphere and attained analytical solutions for the deformation [12]. The finite elastic deformation of hollow circular spheres and cylinders under applied uniform internal pressure was studied by Chung et al[13]. Erbay and Demiray [14] considered the finite axisymmetric deformation of a circular cylindrical tube of neo-Hookean material by using an asymptotic expansion method. Their perturbation solution is founded on the smallness of the ratio of thickness to inner radius of the tube. Normal and tangential tractions were applied on the inner surface of the tube but no boundary conditions were considered at the ends of the tube. Heil [15] and Marzo [16] performed a numerical simulation of the post-buckling behaviour of tubes under external pressure. Finite axisymmetric deformations of thick-walled carbon-black filled rubber tubes were also studied experimentally by Beatty and Dadras [17]. They found that for aspect ratios less than 5 tubes exhibit radially or axially symmetric bulging modes of deformation, distinct from the familiar Euler buckling that occurs for longer tubes. Significantly, they found that the experimentally observed critical compression load is considerably lower than that predicted on the basis of the linear theory. Zhu et. al studied Asymmetric bifurcations of thick-walled circular cylindrical elastic tubes under axial loading and external pressure[18]. The same authors also investigated nonlinear axisymmetric deformations of an elastic tube under external pressure.[19] In another study behavior of a hyperelastic gas-filled spherical shell in a viscous fluid was studied by Allen and Rashid[20]. The behavior of an inflating spherical membrane investigated to provide information on the pressure-deformation response by Needleman [21], Chen and Healey [22], Müller and Struchtrup [23], Goriely et al. [24], Beatty [25] and Rudykh et al.[26]. Their studies showed that the spherical configuration is maintained during initial inflation up to a pressure maximum. Studying above mentioned researches shows that stress analysis of the thick spherical shell, have not investigated in the above mentioned researches.

The objective of this work is to present an exact analytical solution for stresses and displacements of pressurized thick spheres made of isotropic rubber like materials subjected to internal and external pressure. The mathematical model describes the finite deformation problem for the everted spherical shell. It is assumed that the sphere is deformed statically and maintained sphere during deformation and made of an incompressible neo-Hookean material. In addition, Sensitivity of stress components and stretch to applied pressure and to outer to inner radius ratio of vessel has been investigated, carefully.

2. HYPERELASTICITY

Hyperelasticity is the study of nonlinear elastic materials undergoing large deformation. Rubbers are typically hyperelastic. In hyperelasticity, the stress is not calculated directly from strain as in the case of small strains, linear elastic materials. Instead, stresses are derived from the principle of virtual work using the stored strain energy potential functionW, which is expressed with principal invariants of deformation gradient tensor **F**. The deformation gradient **F** relates quantities before deformations to them after or during deformations. Consider a point at position**X**. If this point is displaced to a new position, then the deformation gradient tensor **F** is defined as:

$$\mathbf{F} = {}^{\partial \mathbf{x}}/_{\partial \mathbf{X}}. \quad (1)$$

The deformation gradient tensor can be decomposed into stretch and rotation parts using polar decomposition:$\mathbf{F} = \mathbf{VR} = \mathbf{RU}$, where $\mathbf{R}$ denotes a proper orthogonal rotation tensor, and $\mathbf{U}$ and $\mathbf{V}$ are the right and left stretch tensors, respectively. The stretch tensors are not convenient measures of strain since they require evaluation by polar decomposition. The right Cauchy-Green tensor $\mathbf{C} = \mathbf{F^T F}$ and the left Cauchy-Green tensor $\mathbf{B} = \mathbf{F F^T}$ are often easier to evaluate. The Lagrangian strain tensor is given by $2\mathbf{E} = (\mathbf{C} - \mathbf{I})$where $\mathbf{I}$ is the identity matrix. A material is said to be path-independent or hyperelastic if the work done by the stresses during the deformation process depends only on its initial configuration at time $\mathrm{t} = 0$ and the final configuration at time t [17]. As a consequence of the path-independence:

$$\mathrm{W} = \int_0^{\mathrm{t}} \mathbf{S}\colon \dot{\mathbf{E}}\mathrm{dt}\,; \dot{\mathrm{W}} = \mathbf{S}\colon \dot{\mathbf{E}} \quad (2)$$

where $\mathbf{S}$ is the second Piola-Kirchhoff stress tensor and $\dot{\mathrm{E}}$ is the time rate of change of the Lagrangian strain tensor. Assume $\mathrm{W} = \mathrm{W}(\mathbf{E}(\mathbf{X}), \mathbf{X})$, then:

$$\dot{\mathrm{W}} = \sum_{\mathrm{i,j}=1}^{3} \frac{\partial \mathrm{W}}{\partial \mathbf{E}_{\mathrm{ij}}} \dot{\mathbf{E}}_{\mathrm{IJ}} \quad (3)$$

Consider the strain energy potential $\mathrm{W} = \mathrm{W}(\mathrm{I}_1, \mathrm{I}_2, \mathrm{I}_3)$, where $\mathrm{I}_1, \mathrm{I}_2, \mathrm{I}_3$ are the first, second and third invariants of B.

$$\mathrm{I}_1 = \mathrm{tr}(\mathbf{B}) = \lambda_1^2 + \lambda_2^2 + \lambda_3^2\,, \mathrm{I}_2 = \frac{1}{2}\left[\mathrm{tr}^2(\mathbf{B}) - \mathrm{tr}\left(\mathbf{B^2}\right)\right] = \lambda_1^2\lambda_2^2 + \lambda_2^2\lambda_3^2 + \lambda_3^2\lambda_1^2, \mathrm{I}_3 = \det \mathbf{B} = \lambda_1^2\lambda_2^2\lambda_3^2 \quad (4)$$

λ_{i} $(\mathrm{i} = 1,2,3)$ are the principal stretches. Constitutive relation for hyperelastic materials is:

$$\mathbf{S} = 2\left[\frac{\partial \mathrm{W}}{\partial \mathrm{I}_1}\mathbf{I} + \frac{\partial \mathrm{W}}{\partial \mathrm{I}_2}(\mathrm{I}_1\mathbf{I} - \mathbf{C}) + \frac{\partial \mathrm{W}}{\partial \mathrm{I}_3}\mathrm{I}_3\mathbf{C}^{-1}\right] \quad (5)$$

Transformation of the second Piola-Kirchhoff stress to Cauchy stress tensor σ gives:

$$\boldsymbol{\sigma} = \frac{1}{\mathrm{J}}\mathbf{F S F^T} \quad (6)$$

Where $\mathrm{J} = \det \mathbf{F}$. Moreover, for incompressible materials like rubbers and rubber-like materials W are only function of the first and the second principle invariants of $\mathbf{B}$.

$$\boldsymbol{\sigma} = -\mathrm{p}\mathbf{I} + 2\mathrm{W}_1\mathbf{B} + 2\mathrm{W}_2(\mathrm{I}_1\mathbf{B} - \mathbf{B}^2) \quad (7)$$

Where W_1 and W_2 are derivatives of W respect I_1 and I_2 respectively. Cauchy stress can also be written in the following form, where Strain energy function W is consideredW $= \hat{\mathrm{w}}(\mathrm{i}_1, \mathrm{i}_2)$ and $\mathrm{i}_1, \mathrm{i}_2$are principal invariant of $\mathbf{V}$

$$\boldsymbol{\sigma} = -\mathrm{p}\mathbf{I} + \hat{\mathrm{w}}_1\mathbf{V} - \hat{\mathrm{w}}_2\mathbf{V^{-1}} \quad (8)$$

Where $\hat{\mathrm{w}}_1$ and $\hat{\mathrm{w}}_2$ are derivatives of $\hat{\mathrm{w}}$ respect i_1 and i_2 respectively. For $\mathrm{W} = \breve{\mathrm{w}}(\lambda_1, \lambda_2, \lambda_3)$ component Cauchy stress can be expressed:

$$\sigma_i = -p + \lambda_i \frac{\partial \bar{w}}{\partial \lambda_i} \text{ (no sum on i)} \quad (9)$$

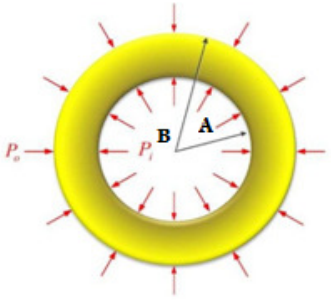

Figure 1. Configuration of hollow sphere

3. PROBLEM FORMULATION

Consider a hollow thick sphere made of rubber like materials with an inner radius A and an outer radius B, subjected to internal and external pressure p_{in} and p_o respectively (Figure. 1).It is assumed that the sphere is deformed statically and material is made of an isotropic and incompressible hyperelastic material. We consider an initially stress-free thick-walled sphere made of rubber like materials. Let (R,Θ,Φ) and (r, θ, φ) be the spherical coordinates in the undeformed and deformed configurations, respectively. In these configurations the geometry of the sphere is described in terms of spherical coordinates:

$$A \le R \le B 0 \le \Theta \le 2\pi 0 \le \Phi \le \pi \quad (10)$$
$$a \le r \le b \qquad 0 \le \theta \le 2\pi 0 \le \varphi \le \pi \quad (11)$$

With the assumption of axially symmetric deformation, the deformation of spherical shell is given by

$$r = r(R), \theta = \Theta, \varphi = \Phi \quad (12)$$

The deformation gradient**F** is given by:

$$\mathbf{F} = \begin{bmatrix} \frac{dr}{dR} & 0 & 0 \\ 0 & \frac{r}{R} & 0 \\ 0 & 0 & \frac{r}{R} \end{bmatrix} \quad (13)$$

Where,$\lambda_r = \frac{dr}{dR}, \lambda_\theta = \lambda_\varphi = \frac{r}{R}$ .In this problem,$\mathbf{R} = \mathbf{I}$, therefore, $\mathbf{V} = \mathbf{F}$**.** the principal invariants of **V** are:

$$i_1 = \frac{dr}{dR} + 2\left(\frac{r}{R}\right)^2 \; i_2 = 2\frac{r}{R}\frac{dr}{dR}^2 + \left(\frac{r}{R}\right)^2 \; i_3 = J = 1 \quad (14)$$

The corresponding left Cauchy–Green deformation tensor is:

$$\mathbf{B} = \mathbf{FF^T} = \begin{bmatrix} \left(\frac{dr}{dR}\right)^2 & 0 & 0 \\ 0 & \left(\frac{r}{R}\right)^2 & 0 \\ 0 & 0 & \left(\frac{r}{R}\right)^2 \end{bmatrix} \quad (15)$$

The principal invariants of the left Cauchy-Green deformation tensor are:

$$I_1 = \left(\frac{dr}{dR}\right)^2 + 2\left(\frac{r}{R}\right)^2 \; I_2 = 2\left(\frac{dr}{dR}\right)^2 \left(\frac{r}{R}\right)^2 + \left(\frac{r}{R}\right)^4 \; I_3 = J^2 = 1 \quad (16)$$

For incompressible materials $I_3 = J^2 = 1$, therefore: $\left(\frac{dr}{dR}\right)\left(\frac{r}{R}\right)^2 = 1$, and radial deformation is calculated:

$$R^3 = r^3 - q \quad (17)$$
$$q = b^3 - B^3 \quad (18)$$

q is a constant which should be calculated by boundary condition. For simplicity, following parameters are defined as:

$$\alpha = \frac{B}{A} \quad ,\lambda_b = \frac{b}{B}, \frac{a}{A} = \left(\alpha^3\left({\lambda_b}^3 - 1\right) + 1\right)^{1/3} \quad (19)$$

According to the principle of conservation of linear momentum, the equilibrium equation of the thick-walled sphere, in the absence of body forces in the radial direction, is expressed as:

$$\frac{d\sigma_r}{dr} + 2\frac{\sigma_r - \sigma_\theta}{r} = 0 \quad (20)$$

Constant uniform radial pressure $p_{in}$and p_o are applied at inner and outer surfaces of the spherical shell. Therefore, the boundary conditions are:

$$\sigma_r(r = a) = -p_{in} \text{ and } \sigma_r(r = b) = -p_o \quad (21)$$

3.1. Formulation for $\mathbf{W = W(I_1, I_2)}$

Where strain energy function W is consideredW $= W(I_1, I_2)$, Cauchy stress tensor is given by:

$$\sigma = -p\begin{bmatrix} 1 & 0 & 0 \\ 0 & 1 & 0 \\ 0 & 0 & 1 \end{bmatrix} + 2W_1\begin{bmatrix} \left(\frac{dr}{dR}\right)^2 & 0 & 0 \\ 0 & \left(\frac{r}{R}\right)^2 & 0 \\ 0 & 0 & \left(\frac{r}{R}\right)^2 \end{bmatrix} + 2W_2\left(\left(\frac{dr}{dR}\right)^2 + 2\left(\frac{r}{R}\right)^2\right)\begin{bmatrix} \left(\frac{dr}{dR}\right)^2 & 0 & 0 \\ 0 & \left(\frac{r}{R}\right)^2 & 0 \\ 0 & 0 & \left(\frac{r}{R}\right)^2 \end{bmatrix} -$$
$$\begin{bmatrix} \left(\frac{dr}{dR}\right)^4 & 0 & 0 \\ 0 & \left(\frac{r}{R}\right)^4 & 0 \\ 0 & 0 & \left(\frac{r}{R}\right)^4 \end{bmatrix} \quad (22)$$

where p is the hydrostatic pressure relating to the incompressibility constraint. Substitute σ_r and σ_θ from equation (22) to equation (20) and integration respect to r yields:

$$\sigma_r = -4\int_a^r \frac{1}{r}\left[W_1\left(\left(\frac{dr}{dR}\right)^2 - \left(\frac{r}{R}\right)^2\right) - W_2\left(\frac{r}{R}\right)^4\right]dr - p_{in} \quad (23)$$

$$\sigma_\theta = \sigma_\varphi = \sigma_r + 2\left[W_1\left(\left(\frac{r}{R}\right)^2 - \left(\frac{dr}{dR}\right)^2\right) + W_2\left(\left(\frac{r}{R}\right)^4 - \left(\frac{dr}{dR}\right)\right)\right] \quad (24)$$

Constants are determined by:

$$-p_o = -4\int_a^b \frac{1}{r}\left[W_1\left(\left(\frac{dr}{dR}\right)^2 - \left(\frac{r}{R}\right)^2\right) - W_2\left(\frac{r}{R}\right)^4\right]dr - p_{in} \quad (25)$$

Maximum shear stress $\sigma_{r\theta} = \sigma_{r\varphi}$is calculated as:

$$\sigma_{r\theta} = \sigma_{r\varphi} = \left|\frac{1}{2}(\sigma_r - \sigma_\theta)\right| = \left|\frac{1}{2}(\sigma_r - \sigma_\varphi)\right| = W_1\left(\left(\frac{R}{r}\right)^4 - \left(\frac{r}{R}\right)^2\right) + W_2\left(\left(\frac{R}{r}\right)^2 - \left(\frac{r}{R}\right)^4\right) \quad (26)$$

In the solid sphere with pressure applied on the outer surface, the center of sphere can not move radially (because of symmetry, deformation), therefore q=0, and $R^3 = r^3$. In this case:

$$\sigma_r = -p + 2W_1\left(\frac{dr}{dR}\right)^2 + 2W_2\left(\frac{dr}{dR}\right) \quad (27)$$

$$\sigma_\theta = \sigma_\varphi = -p + 2W_1\left(\frac{r}{R}\right)^2 + 2W_2\left(\frac{dr}{dR} + \left(\frac{r}{R}\right)^4\right) \quad (28)$$

By considering$\sigma_r(r = r_o) = -p_o$, hydrostatic pressure is given by:

$$p = p_o + 2W_1\left(\frac{R_o}{r_o}\right)^4 + 2W_2\left(\frac{R_o}{r_o}\right) \quad (29)$$

and stress component is:

$$\sigma_r = -p_o + 2W_1\left(\left(\frac{dr}{dR}\right)^2 - \left(\frac{R_o}{r_o}\right)^4\right) + 2W_2\left(\frac{dr}{dR} - \left(\frac{R_o}{r_o}\right)\right) \quad (30)$$

$$\sigma_\theta = \sigma_\varphi = -p_o + 2W_1\left(\left(\frac{r}{R}\right)^2 - \left(\frac{R_o}{r_o}\right)^4\right) + 2W_2\left(\frac{dr}{dR} + \left(\frac{r}{R}\right)^4 - \left(\frac{R_o}{r_o}\right)\right) \quad (31)$$

3.1.1.Case Study: Neo-Hookean Strain Energy Function

Neo-Hookean strain energy function for incompressible materials is as follows:

$$W = \mu(I_1 - 3) \quad (32)$$

Therefore:$W_1 = \mu$ and equation (23) by considering incompressibility condition becomes:

$$\sigma_r = 4\int_a^r \left[\mu\left(\frac{r^6 - R^6}{r^5 R^2}\right)\right]dr - p_{in} \quad (33)$$

By integration of above equation, stress components are achieved:

$$\sigma_r = \mu\left(\left[5\left(\frac{R}{r} - \frac{A}{a}\right)\right] - q\left[\frac{R}{r^4} - \frac{A}{a^4}\right]\right) - p_{in} \quad (34)$$

$$\sigma_\theta = \sigma_\varphi = \mu\left(\left[5\left(\frac{R}{r}-\frac{A}{a}\right)\right] - q\left[\frac{R}{r^4}-\frac{A}{a^4}\right] + 2\left[\left(\frac{r}{R}\right)^2 - \left(\frac{R}{r}\right)^4\right]\right) \quad (35)$$

Second boundary condition is used to findλ_b. Therefore:

$$\frac{p_i - p_o}{\mu} = 4\left(\frac{1}{\lambda_b} - \frac{1}{\left(a^3\left({\lambda_b}^3-1\right)+1\right)^{1/3}}\right) + \frac{1}{{\lambda_b}^4} - \frac{1}{\left(a^3\left({\lambda_b}^3-1\right)+1\right)^{4/3}} \quad (36)$$

Maximum shear stress $\sigma_{r\theta} = \sigma_{r\varphi}$is calculated as:

$$\sigma_{r\theta} = \sigma_{r\varphi} = \left|\frac{1}{2}(\sigma_r - \sigma_\theta)\right| = \left|\frac{1}{2}(\sigma_r - \sigma_\varphi)\right| = \left[\mu\left(\left(\frac{r}{R}\right)^2 - \left(\frac{R}{r}\right)^4\right)\right] \quad (37)$$

In the case of $p_i = 0$, stress is given by:

$$\sigma_r = \mu\left(\left[5\left(\frac{R}{r}-\frac{A}{a}\right)\right] - q\left[\frac{R}{r^4}-\frac{A}{a^4}\right]\right) - p_{in} \quad (38)$$

$$\frac{-p_o}{\mu} = 4\left(\frac{1}{\lambda_b} - \frac{1}{\left(\alpha^3\left({\lambda_b}^3-1\right)+1\right)^{1/3}}\right) + \frac{1}{{\lambda_b}^4} - \frac{1}{\left(\alpha^3\left({\lambda_b}^3-1\right)+1\right)^{4/3}} \quad (39)$$

$$\sigma_\theta = \sigma_\varphi = \mu\left(\left[5\left(\frac{R}{r}-\frac{A}{a}\right)\right] - q\left[\frac{R}{r^4}-\frac{A}{a^4}\right] + 2\left[\left(\frac{r}{R}\right)^2 - \left(\frac{r}{R}\right)^4\right]\right) \quad (40)$$

In the case of $p_o = 0$, stress is given by:

$$\sigma_r = \mu\left(\left[5\left(\frac{R}{r}-\frac{A}{a}\right)\right] - q\left[\frac{R}{r^4}-\frac{A}{a^4}\right]\right) - p_{in} \quad (41)$$

$$\frac{p_i}{\mu} = 4\left(\frac{1}{\lambda_b} - \frac{1}{\left(\alpha^3\left({\lambda_b}^3-1\right)+1\right)^{1/3}}\right) + \frac{1}{{\lambda_b}^4} - \frac{1}{\left(\alpha^3\left({\lambda_b}^3-1\right)+1\right)^{4/3}} \quad (42)$$

$$\sigma_\theta = \sigma_\varphi = \mu\left(\left[5\left(\frac{R}{r}-\frac{A}{a}\right)\right] - q\left[\frac{R}{r^4}-\frac{A}{a^4}\right] + 2\left[\left(\frac{r}{R}\right)^2 - \left(\frac{r}{R}\right)^4\right]\right) - p_{in} \quad (43)$$

In the solid sphere with pressure applied on the outer surface:

$$\sigma_r = -p_o + 2\mu\left(\left(\frac{dr}{dR}\right)^2 - \left(\frac{R_o}{r_o}\right)^4\right) \quad (44)$$

$$\sigma_\theta = \sigma_\varphi = -p_o + 2\mu\left(\left(\frac{r}{R}\right)^2 - \left(\frac{R_o}{r_o}\right)^4\right) \quad (45)$$

σ_r is a function of r and its maximum occurs when:$\frac{d\sigma_r}{dr} = 0$. Critical point for σ_r are $r = \left(\frac{q}{2}\right)^{\frac{1}{3}} = \frac{A}{2}\left(\alpha^3\left({\lambda_b}^3-1\right)\right)^{1/3}$, $r = 0$ and $r = (q)^{\frac{1}{3}} = A\left(\alpha^3\left({\lambda_b}^3-1\right)\right)^{1/3}$.

4. RESULT AND DISCUSSION

Material constant "μ" is determined by using Levenberg–Marquardt nonlinearregression method for the rubber tested by Trelore [27] and μ=0.398 is achieved by numerical calculation and comparison with experimental data.

Example 1: A spherical shell with inner and outer radius A = 1 m, B = 2 m is considered in this case. The applied internal pressure p_{in} varies from $\frac{p_{in}}{\mu} = -0.1$ to $\frac{p_{in}}{\mu} = -1.6$. Equation (36) will be solved for λ_b by considering $\alpha = 2$ and for different values of $\frac{p_{in}}{\mu}$.

Figure.2 shows the distribution of Extension ratio through the thickness for different internal pressure. Extension ratio is maximum in the inner radius where body subjected to internal pressure. It decreases through the thickness and is minimum in the outer radius which is a stress free surface. Moreover, extension ratio in each arbitrary radius increases by increasing internal pressure. Differences between extension ratios for different internal pressure decrease through the thickness. In addition, the ratio of extension ratios of different pressure decreases through the thickness. In the inner radius λ for $\frac{p_{in}}{\mu} = -1.6$ is 1.619 λ for $\frac{p_{in}}{\mu} = -0.1$ but λ in the outer surface for $\frac{p_{in}}{\mu} = -1.6$ it is only 1.124 λ for $\frac{p_{in}}{\mu} = -0.1$. Effect of pressure on extension ratio at different radius is illustrated in Figure. 3. It shows that in specific internal pressure, extension ratio decreases by increasing the distance from inner surface.

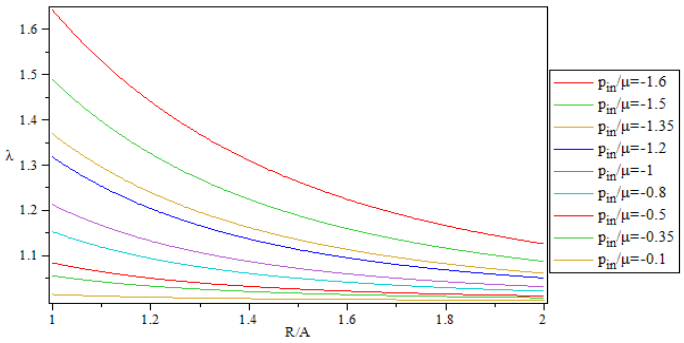

Figure 2. Distribution of Extension ratio through the thickness for different internal pressure and $\frac{B}{A} = 2$

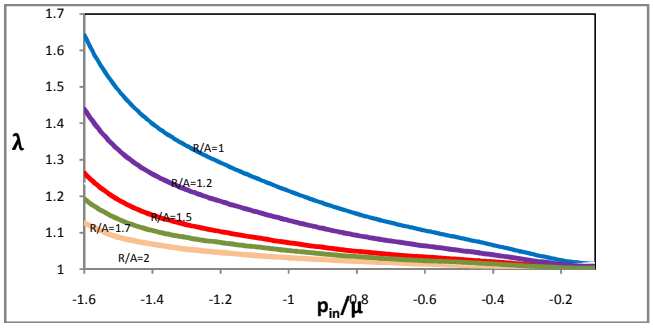

Figure 3. Extension ratio versus internal pressure at different undeformed radius and $\frac{B}{A} = 2$

Figure.4 illustrates radius of sphere in the current configuration versus radius of sphere in the reference configuration for different internal pressure. Variation of current radius versus internal pressure is shown in Figure.5. Ratio of outer radius to inner radius decreases by increasing pressure. This ratio is 1.975 for $\frac{p_{in}}{\mu} = -0.1$ and it is only 1.371 for $\frac{p_{in}}{\mu} = -1.6$.

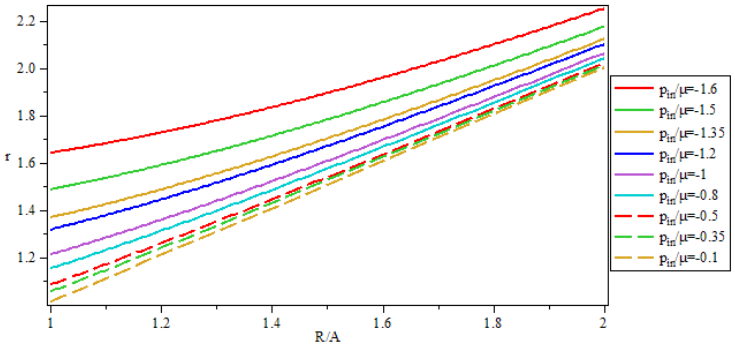

Figure 4. Radius of sphere in the current configuration versus radius of sphere in the reference configuration for different internal pressure and $\frac{B}{A} = 2$

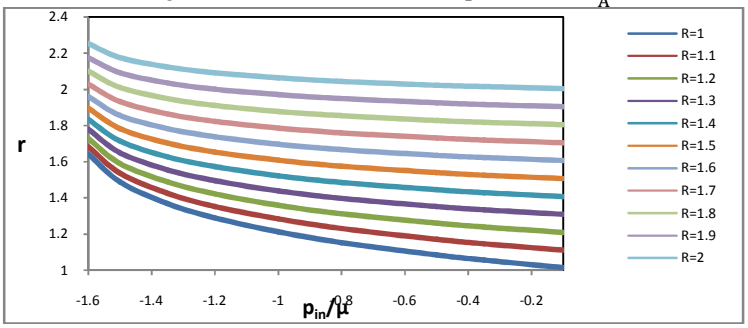

Figure 5. Radius of sphere in the current configuration versus internal pressure at different undeformed radius and $\frac{B}{A} = 2$

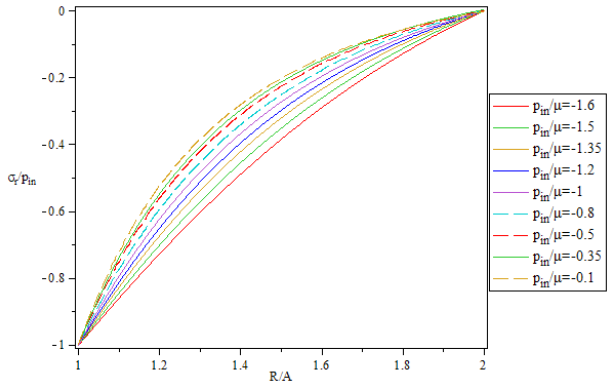

Figure 6. .Distribution of Normalized radial stress through the thickness for different internal pressure and $\frac{B}{A} = 2$

Distribution of Normalized radial stress through the thickness for different internal pressure is shown in Figure.6. Normalized radial stress in specific radius decreases by decreasing pressure. At points away from the boundaries, normalized radial stress shows significant differences for different pressures, while at points near the boundaries, the reverse holds true. In Figure. 7 distribution of Normalized radial stress versus internal pressure at different undeformed radius is presented. Stress decreases by increasing radius in specific pressure. it is also observed that Normalized radial stress is more sensitive to pressure in lower radius. Distribution of Normalized radial stress versus extension ratio at different internal pressure is shown in Figure. 8.

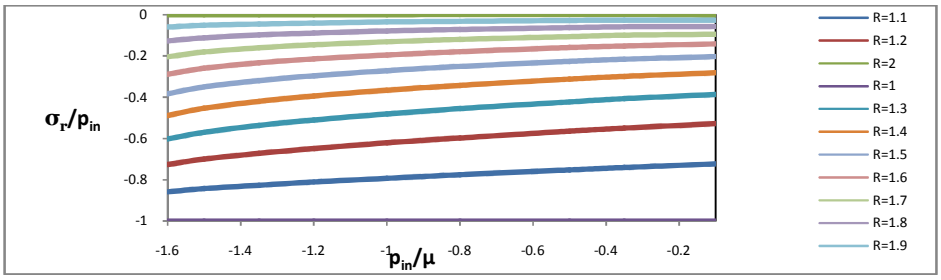

Figure 7. Distribution of Normalized radial stress versus internal pressure at different undeformed radius and $\frac{B}{A} = 2$

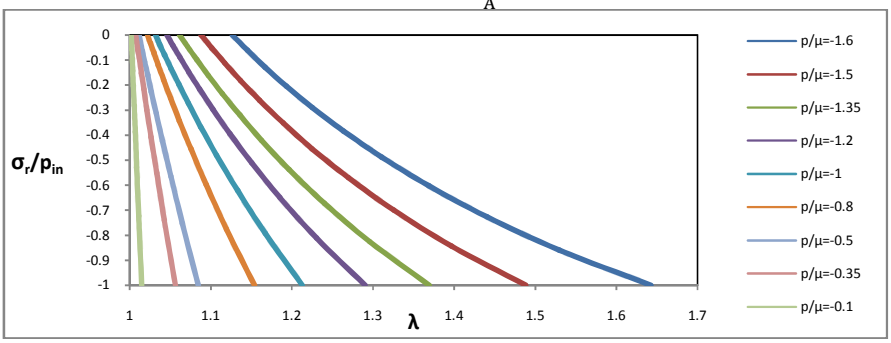

Figure 8. Distribution of Normalized radial stress versus extension ratio at different internal pressure and $\frac{B}{A} = 2$

In Figure. 9 Distribution of Normalized hoop stress versus radius at different pressure is presented. Normalized hoop stress decreases by increasing radius. Moreover, it is maximum in the inner radius and minimum in the outer radius in specific pressure. Differences between normalized hoop stresses in inner radius for different pressure are much greater than the differences in the outer surface. Additionally, Distribution of Normalized hoop stress versus internal pressure at different undeformed radius is presented in Figure. 10. This shows that normalized hoop stress decreases when the applied internal pressure decreases. Besides, in high internal pressure normalized hoop stress decreases rapidly through the thickness in comparison with low pressure. Figure. 11 and 12 present distributions of Normalized maximum shear stress through the thickness for different internal pressure and Normalized maximum shear stress versus internal pressure at different undeformed radius. Normalized maximum shear stress has the same distribution as normalized hoop stress.

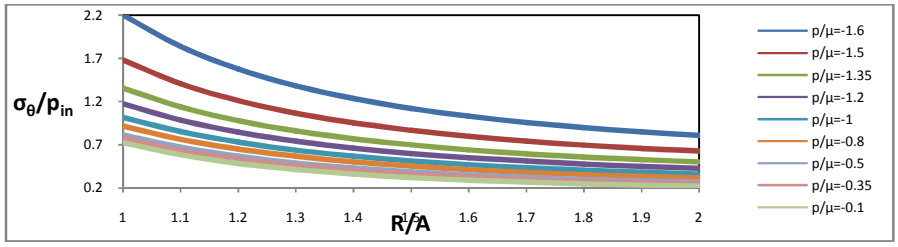

Figure 9. Distribution of Normalized hoop stress through the thickness for different internal pressure and $\frac{B}{A} = 2$

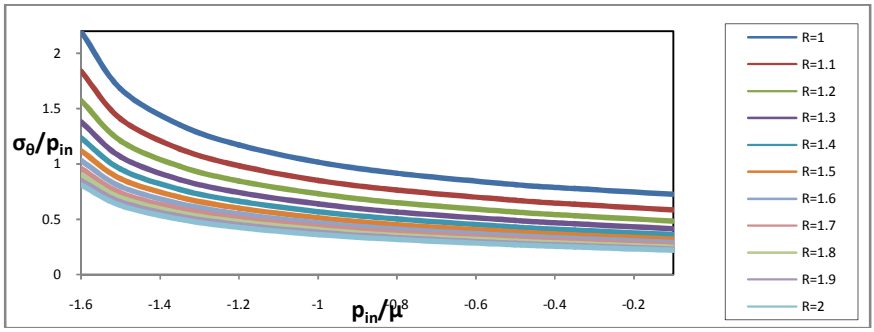

Figure 10. Distribution of Normalized hoop stress versus internal pressure at different undeformed radius and $\frac{B}{A} = 2$

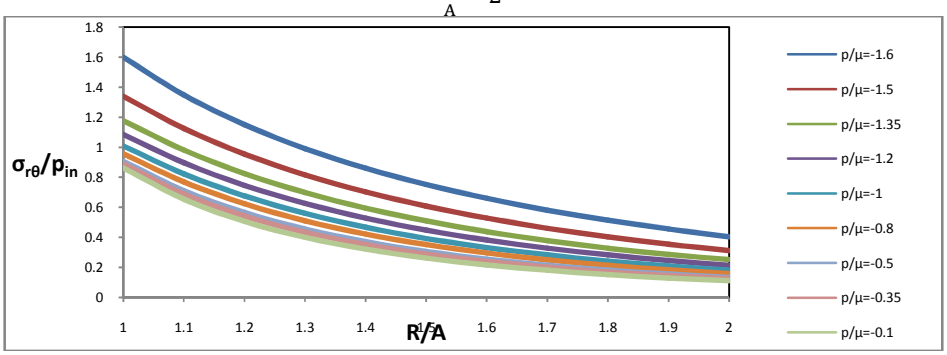

Figure 11. Distribution of Normalized maximum shear stress through the thickness for different internal pressure and $\frac{B}{A} = 2$

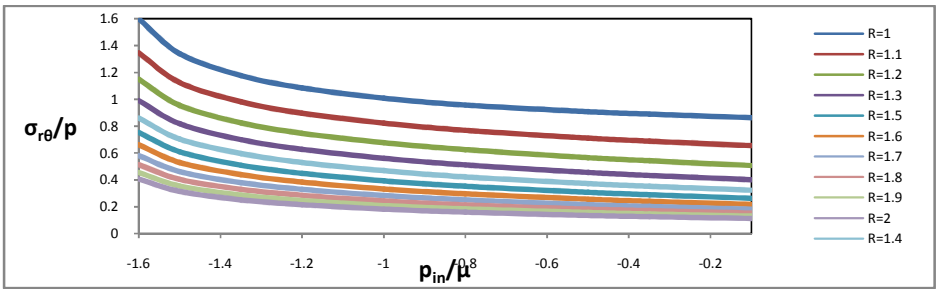

Figure 12. Distribution of Normalized maximum shear stress versus internal pressure at different undeformed radius and $\frac{B}{A} = 2$

In this study, in order to do a numerical analysis of the problem, a geometry specimen was modeled using a commercial finite elements code, Abacus 6.12, for a comparative study. In the FE model, due to symmetry, only a half of the sphere specimen geometry was considered. An 8-node linear brick, reduced integration with hourglass control, hybrid with constant pressure(C3D8RH) is used. Figure. 13 illustrates the meshing region. The nodal points along the vertical edge passing through the center were free to move in radial direction but were constrained from moving in the circumferential direction to reflect the symmetry of sphere specimen geometry. In the finite element model input data are as the same as considered in the example.1 and the same result is obtained by FEM model for stress components. The displacement and stresses distributions are compared with

the solutions of the finite element method (FEM) and good agreement was found. Results are presented in Figure. 14 and 15.

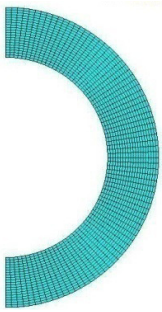

Figure 13. . Finite element mesh region.

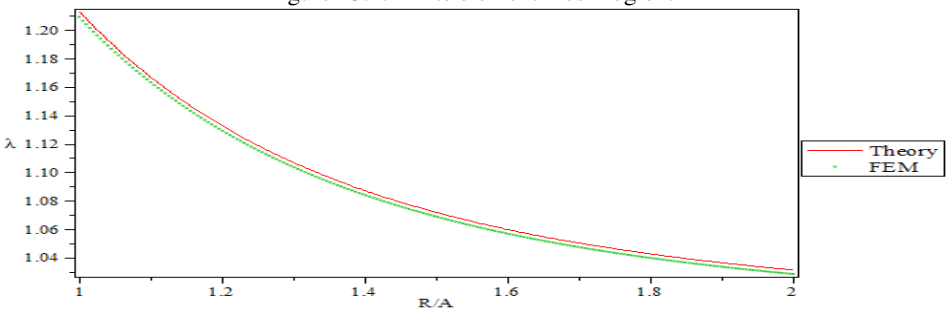

Figure 14. Comparison of theory and FEM results for extension ratio for $\frac{B}{A} = 2 \& \frac{p_{in}}{\mu} = -1$

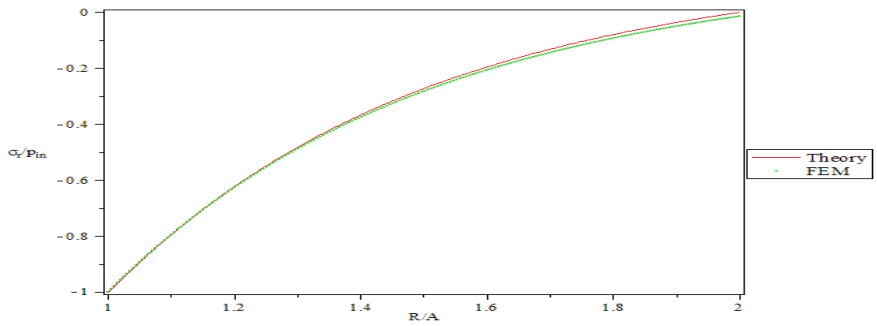

Figure 15. Comparison of theory and FEM results for radial stress for $\frac{B}{A} = 2 \& \frac{p_{in}}{\mu} = -1$

Example 2: A spherical shell with inner and outer radius $A = 1$ m, $B = 5$ m is considered in this case. The applied internal pressure p_i varies from $\frac{p_{in}}{\mu} = -0.1$ to $\frac{p_{in}}{\mu} = -3$. Equation (36) has been solved for λ_b by considering $\alpha = 5$ and for different values of $\frac{p_{in}}{\mu}$. In Figure. 16-20 distribution of extension ratio, deformed radius, normalized radial stress and normalized hoop stress versus undeformed radius are presented for this example. Following results are obtained from the comparison of the graphs of this example and previous one. Distribution of above mentioned parameters has the same trend for both examples. However, the thicker vessel demonstrates lower extension ratio in the inner surface for the same pressure. The same result is achieved for deformed internal radius, normalized hoop stress and normalized shear stress. Comparison of Normalized radial stress of two vessels shows that it varies slightly for thinner vessel than the thicker one. Even so, in the same radius normalized radial stress for the thicker vessel is greater. For example,

normalized radial stress is 0.3 for this example and 0.2 for the previous example at $\frac{R}{A} = 1.5$ and $\frac{p_{in}}{\mu} = -1$.

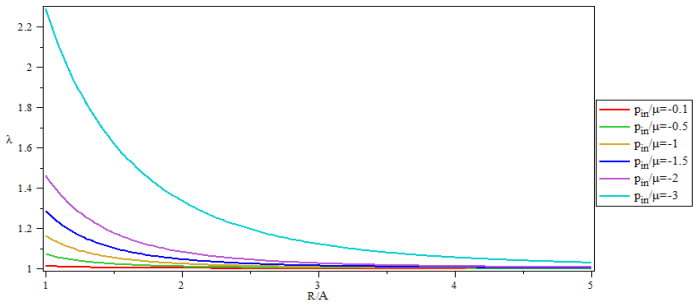

Figure 16. Distribution of Extension ratio through the thickness for different internal pressure and $\frac{B}{A} = 5$

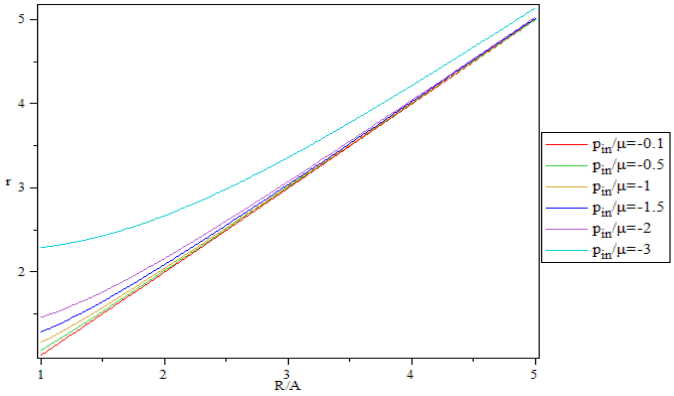

Figure 17. . Radius of sphere in the current configuration versus radius of sphere in the reference configuration for different internal pressure and $\frac{B}{A} = 5$

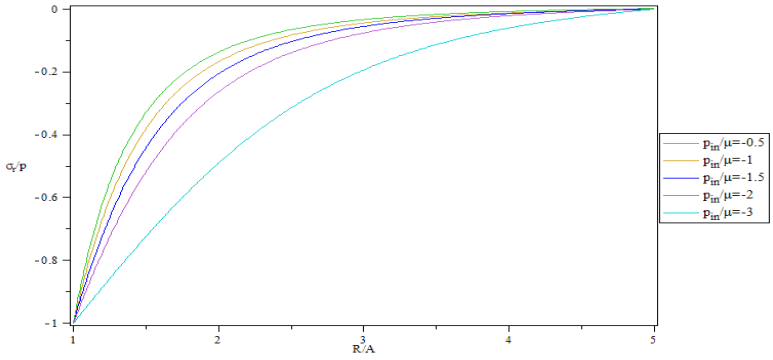

Figure 18. Distribution of Normalized radial stress through the thickness for different internal pressure and $\frac{B}{A} = 5$

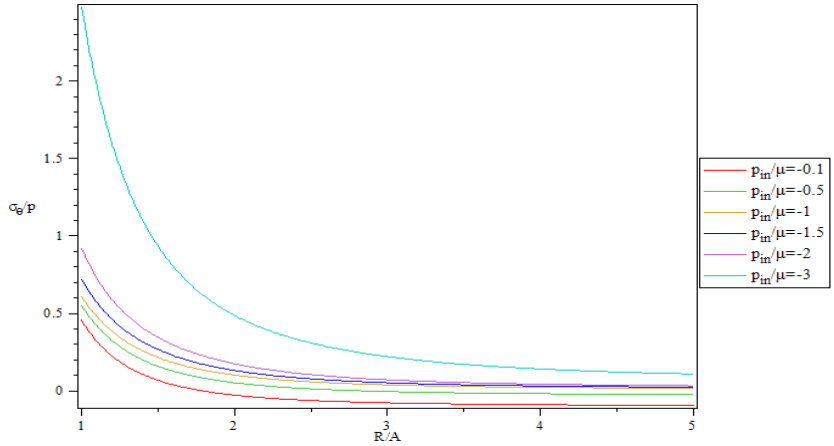

Figure 19. Distribution of Normalized hoop stress through the thickness for different internal pressure and $\frac{B}{A} = 5$

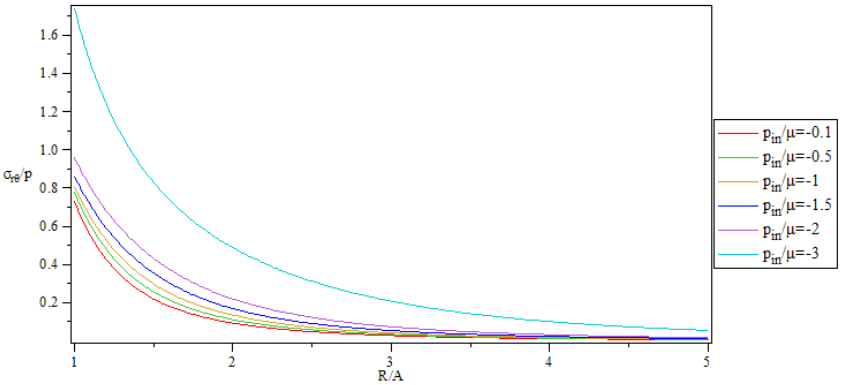

Figure 20. Distribution of Normalized maximum shear stress through the thickness for different internal pressure and $\frac{B}{A} = 5$

Example 3: A spherical shell with inner and outer radius A = 1 m, B = 2m is considered in this case. The applied external pressure p_o varies from $\frac{p_o}{\mu} = -0.1$ to $\frac{p_o}{\mu} = -5$. Equation (36) will be solved for λ_b by considering $\alpha = 2$ and for different values of $\frac{p_o}{\mu}$.

Figure. 21 shows the distribution of Extension ratio through the thickness for different internal pressure. Extension ratio is minimum in the inner radius then it increases through the thickness and is maximum in the outer radius which is subjected to external pressure. Extension ratio in an arbitrary radius decreases by increasing internal pressure. Ratio of λ for different external pressures in each radius decreases through the thickness. For example, in the inner radius λ of $\frac{p_o}{\mu} = -5$ is 0.699 λ of $\frac{p_o}{\mu} = -0.1$ but in the outer surface extension ratio for $\frac{p_o}{\mu} = -5$ is 0.973 extension ratio of $\frac{p_o}{\mu} = -0.1$. The effect of pressure on extension ratio at different radius is illustrated in Figure. 22, which shows that in a specific external pressure extension ratio increases by increasing the distance from inner surface. Figure. 23 illustrates Radius of sphere in the current configuration versus radius of sphere in the reference configuration for different internal pressure. The

observations bring about that that ratio of outer radius to inner radius increases by increasing pressure. This ratio is 2.819 for $\frac{p_o}{\mu} = -5$ and it is only 2.025 for $\frac{p_o}{\mu} = -0.1$.

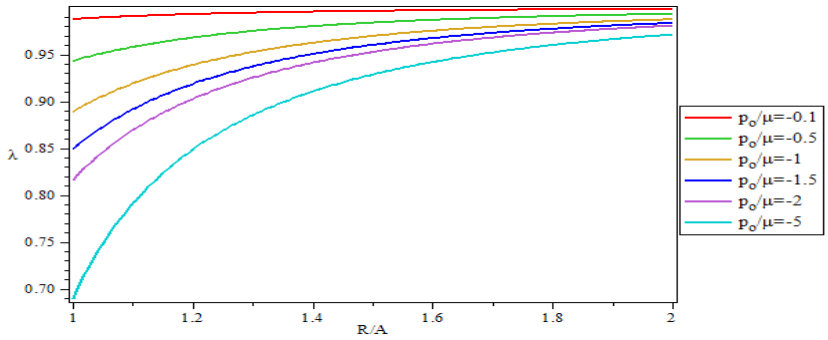

Figure 21. Distribution of Extension ratio through the thickness for different external pressure and $\frac{B}{A} = 2$

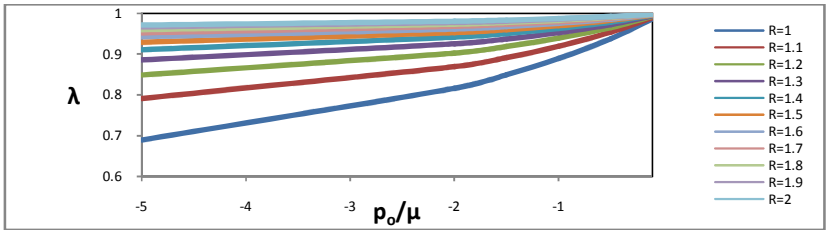

Figure 22. Extension ratio versus external pressure at different undeformed radius and $\frac{B}{A} = 2$

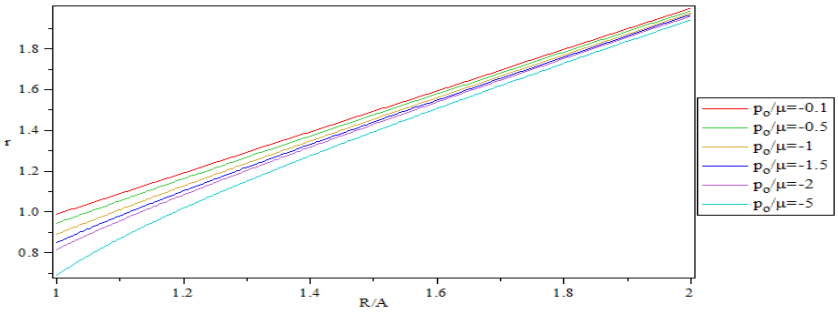

Figure 23. Radius of sphere in the current configuration versus radius of sphere in the reference configuration for different external pressure and $\frac{B}{A} = 2$

Distribution of Normalized radial stress through the thickness for different external pressure is shown in Figure. 24. Normalized radial stress in each radius increases by increasing pressure. At points away from the boundaries, normalized radial stress shows significant differences for different pressures, while at points near the boundaries, the reverse holds true. In Figure. 25 Distribution of Normalized radial stress versus internal pressure at different undeformed radius is presented. Radial

stress increases by increasing radius in specific pressure. Also it is observed that Normalized radial stress is more sensitive to pressure in lower radius.

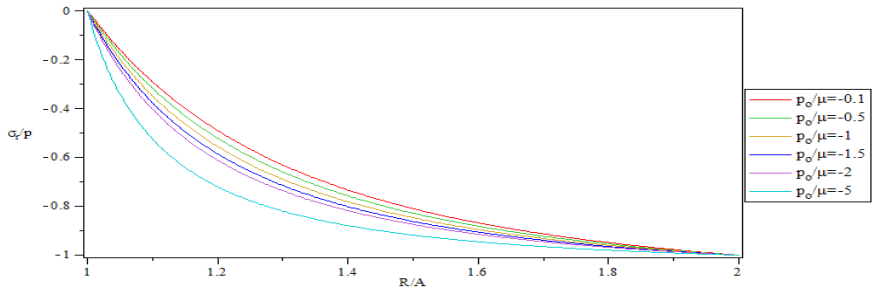

Figure 24. Distribution of Normalized radial stress through the thickness for different external pressure and $\frac{B}{A} = 2$

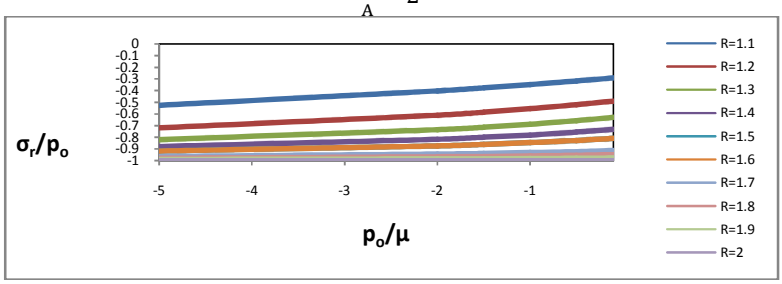

Figure 25. Distribution of Normalized radial stress versus external pressure at different undeformed radius and $\frac{B}{A} = 2$

Figure. 26 presents distribution of Normalized hoop stress versus undeformed radius at different external pressure. Normalized hoop stress decreases by increasing radius. Moreover, it is maximum in the inner radius and minimum in the outer radius in an arbitrary pressure. Distribution of Normalized hoop stress versus internal pressure at different undeformed radius is presented in Figure. 27. It is observed that normalized hoop stress increases when the applied external pressure increases. Figure.28 is the graph of Distribution of Normalized maximum shear stress through the thickness for different internal pressure. Normalized maximum shear stress has the same distribution as normalized hoop stress.

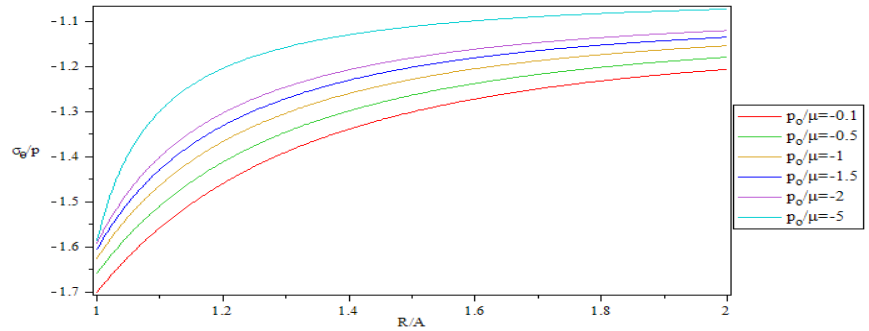

Figure 26. Distribution of Normalized hoop stress through the thickness for different external pressure and $\frac{B}{A} = 2$

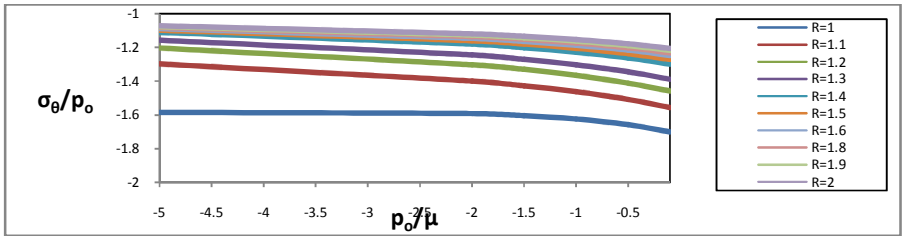

Figure 27. Distribution of Normalized hoop stress versus external pressure at different undeformed radius and $\frac{B}{A} = 2$

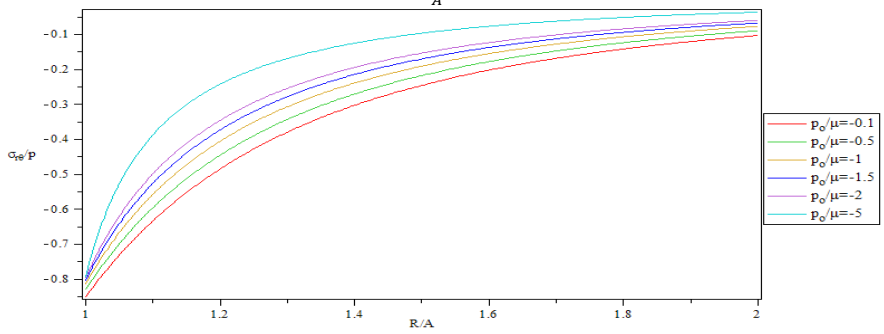

Figure 28. . Distribution of Normalized maximum shear stress through the thickness for different external pressure and $\frac{B}{A} = 2$

4. CONCLUSION

Stresses and displacements in thick-walled spherical shells made of isotropic homogenous hyperelastic materials subjected to internal and external pressure are developed by an analytical method. Neo-hookean strain energy function is used to find stress and displacement for the sphere in different pressures and material constant is calculated from experimental data by numerical method. Effect of outer to inner radius ratio in stress and displacement is studied. In each pressure, stress and displacement for different radius is calculated. The displacement and stresses distributions are compared with the solutions of the finite element method (FEM) and good agreement was found. Results show that value of outer to inner radius ratio has a great effect on deformations and stresses and is a useful parameter from a design point of view which can be tailored to specific applications to control the stress. It is also possible to find an optimum value for the mentioned ratio which the variation of stresses along the radial direction is minimized, yielding optimum use of material.

REFERENCES:

[1] Beatty,M.F., (1987) "Topics in finite elasticity: hyperelasticity of rubber, elastomers, and biological tissues—with examples",App. Mech. Rev., Vol.40, No.5,pp1699 -1735.

[2] Horgan,C.O. &Polignone,D.A.,(1995)"Cavitation in nonlinearly elastic solids: A review",App. Mech. Rev.,Vol.48, No.8, pp471-485.

[3] Attard,M.M.,(2003)"Finite strain-isotropic hyperelasticity",Int. J. Solids Struct., Vol.40, No.17, pp 4353-4378.

[4] Fu,Y.B.&Ogden,R.W.,(2001),Nonlinear Elasticity, Cambridge University Press.

[5] Bahreman, M. &Darijani, H., (2015),"New polynomial strain energy function; application to rubbery circular cylinders under finite extension and torsion",J. Appl.Polym. Sci., 132, 41718, doi: 10.1002/app.41718
[6] Carroll, M.M., (2011) , "A strain energy function for vulcanized rubbers",J. Elast., Vol.103, pp. 173-187
[7] Drozdov, A.D., (2007),"Constitutive equations in finite elasticity of rubbers"Int. J. Solids Struct., Vol. 44, pp. 272-297.
[8] Steinmann, P., Mokarram, H., Gunnar, P.(2010), "Hyperelastic models for rubber-like materials: consistent tangent operators and suitability for Treloar's data",Arch. Appl. Mech.,Vol.82, No.9, pp.1183-1217
[9] Reddy, J.N. (2007),"Theory and Analysis of Elastic Plates and Shells, Boca Raton": CRC Press, 403p.
[10] Rivlin, R.S.(1949), "Large elastic deformations of isotropic materials, VI: further results in the theory of torsion, shear and flexure", Philos. Trans. R. Soc., Vol.242,pp. 173–195.
[11] Haghton, D.M.,(1987)"Inflation and Bifurcation of Thick-Walled Compressible ElasticSpherical Shells", J. App. Mech., Vol. 39. pp 259-272.
[12] Abeyakatne, R., &Horgan, C. O. (1984)"The pressurized hollow sphere problem infinite elastostatics for a class of compressible materials", Int. J. Solids Struct., Vol. 20, pp.715-723.
[13] Chung, D.T., Horgan, C.O. &Abeyaratne, R.(1986), "The finite deformation of internally pressurized hollow cylinder and sphere for a class of compressible elastic materials", Int. J. Solids Struct., Vol.12,No.12, pp 1557-1570.
[14] Erbay, H.A. &Demiray, H., (1995)"Finite axisymmetric deformations of elastic tubes: An approximate method". J Eng. Math., Vol. 29, pp 451-472
[15] Heil, M.&Pedley, J.,(1995), "Large axisymmetric deformation of a cylindrical shell conveying a viscous flow",J Flui.Struct.,Vol. 9, pp 237-256.
[16] Marzo,A., Luo, X.Y.&Bertram C.D.(2005),"Three-dimensional collapse and steady flow in thick-walled flexible tubesJ Flui. Struct.,Vol.20, pp 817-835.
[17] Beatty , M.F. &Dadras, P.(1968)," Some experiments on the elastic stability of some highlyelastic bodies". Int.J. Eng. Sci., Vol.14, pp233-238.
[18] Zhu, Y., Luo,X.Y., &Ogden R.W.(2008),"Asymmetric bifurcations of thick-walled circularcylindrical elastic tubes under axial loading and external pressure",Int. J. Solids Struct., Vol.45, pp 3410-3429.
[19] Zhu, Y., Luo, X.Y., &Ogden R.W.(2009),"Nonlinear axisymmetric deformations of an elastic tube under external pressure",European J. of Mech. - A/Solids, Elsevier,Vol. 29, NO. 2, pp.216-229.
[20] Allen, J.S.& Rashid, M.M., (2004)"behavior of a hyperelastic gas-filled spherical shell in aviscous fluid", J. App. Mech., Vol.71, No.2, pp195-200
[21] Needleman, A., (1977),"Inflation of spherical rubber balloons",Int. J. Solids Struct.Vol. 13, pp 409–421.
[22] Chen, Y.C., Healey, T.J., (1991)"Bifurcation to pear-shaped equilibria of pressurizedspherical membranes.". Int. J. Nonlinear Mech., Vol. 26, pp279–291.
[23] Müller, I., Struchtrup, H.,(2002). "Inflating a rubber balloon". Math. Mech. Solids, Vol. 7, pp 569–577.
[24] Goriely, A., Destrade, M., Ben Amar, M., (2006),"Stability and bifurcation of compressed elastic cylindrical tubes."Q. J. Mech. Appl. Math. Vol. 59, pp 615–630.
[25] Beatty, M.F., (2011), "Small amplitude radial oscillations of an incompressible, isotropic elastic spherical shell". Math. Mech. SolidsVol. 16, pp 492–512.
[26] Rudykh, S., Bhattacharya, K., deBotton, G., (2012),"Snap-through actuation of thickwalledelectroactive balloons". Int. J. Nonlinear Mech., Vol. 47, pp206–209.
[27] Treloar, L.R.G., (1944), "Stress-strain data for vulcanised rubber under various types of deformation", Trans. Faraday Soc., Vol. 40, pp 59–70

AUTHORS

Yavar Anani received the BSc degree in mechanical engineering from Amir Kabir University of technology (AUT). He received the MSc in mechanical engineering from Sharif University of Technology (SUT) and now he is PhD student in mechanical Engineering. His research interests are Nonlinear elasticity, Continuum mechanic,

Hyperelasticity, FEM, Plasticity and Thermoelasticity.

GholamhoseinRahimiis professor of solid mechanics in TarbiatModares University(TMU). He received the PhD degree in mechanical engineering from UMIST(England)). His research interests are Plate and shell theory, Continuum mechanic,Hyperelastic Materials, FEM, Plasticity and application of advancematerial in mechanical structures.